Fabrication and electrochemical properties of carbon nanotube/polypyrrole composite film electrodes with controlled pore size

Ji-Young Kim [a], Kwang Heon Kim [a], Kwang Bum Kim [a,b,∗]

[a] *Division of Materials Science and Engineering, Yonsei University, 134 Shinchon Dong, Seodaemoon-gu, Seoul 120-749, Republic of Korea*
[b] *Center for Advanced Materials Processing, 66 Sangnam-Dong, Changwon, Geongsangnam-Do 641-010, Republic of Korea*

Abstract

Carbon nanotube (CNT)/polypyrrole (PPy) composites with controlled pore size in a three-dimensional entangled structure of a CNT film are prepared as electrode materials for a pseudocapacitor. A CNT film electrode containing nanosize silica between the CNTs is first fabricated using an electrostatic spray deposition of a mixed suspension of CNTs and nanosize silica on to a platinum-coated silicon wafer. Later, nanosize silica is removed leaving a three-dimensional entangled structure of a CNT film. Before removal of the silica from the CNT/silica film electrode, PPy is electrochemically deposited on to the CNTs to anchor them in their entangled structure. Control of the pore size of the final CNT/PPy composite film can be achieved by changing the amount of silica in the mixed suspension of CNTs and nanosize silica. Nanosize silica acts as a sacrificial filler to change the pore size of the entangled CNT film. Scanning electron microscopy of the electrochemically prepared PPy on the CNT film substrate shows that the PPy nucleated heterogeneously and deposited on the surface of the CNTs. The specific capacitance and rate capability of the CNT/PPy composite electrode with a heavy loading of PPy of around 80 wt.% can be improved when it is made to have a three-dimensional network of entangled CNTs with interconnected pores through pore size control.
© 2007 Elsevier B.V. All rights reserved.

Keywords: Carbon nanotubes; Polypyrrole; Pore size; Nanosize silica; Nanoporous structure; Specific capacitance

1. Introduction

Currently, electrochemical capacitors (ECs) are attracting much attention for use in high power energy-storage devices. Potential applications of electrochemical capacitors include power enhancement and primary or hybrid power sources combined with batteries and fuel cells for use in hybrid electric vehicles (HEV) or fuel cell electric vehicle (FCEV) propulsion [1,2]. In these ECs, the energy stored is either capacitive or pseudocapacitive in nature. The capacitive or non-Faradaic process is based on charge separation at the electrode/solution interface; whereas the pseudocapacitive process consists of Faradaic redox reactions that occur within the active electrode materials. The most widely used active electrode materials are carbon, conducting polymers, and transition metal oxides [3–13].

Among conducting polymers, polypyrrole (PPy) is by far the most extensively studied on account of the monomer (pyrrole) being easily oxidized, water soluble, and commercially available [9–15]. Swelling/shrinkage of conducting polymers has been pointed out to cause electrode degradation because of the volume change of the polymer in the course of insertion/desertion of counter ions into the polymer during cycling [16]. This is directly related to the cycle-life of conducting polymer-based supercapacitors [17]. Adding carbon, especially carbon nanotubes (CNTs), reportedly is used to improve the mechanical and electrochemical properties of electrodes based on pseudocapacitance materials [18–20]. Moreover, the presence of carbon in the bulk of the conducting polymers provides good electronic conductivity in the electrode. Wu et al. [20] found that the electrical conductivity of 3 wt.% multiwalled carbon nanotube (MWNT)/PPy composites was about 150% higher than that of PPy without MWNTs at room temperature.

CNTs have uniform diameters of several tens of nanometers and have unique properties such as a three-dimensional entangled structure on the nanometer scale. When a conduct-

∗ Corresponding author at: Division of Materials Science and Engineering, Yonsei University, 134 Shinchon Dong, Seodaemoon-gu, Seoul 120-749, Republic of Korea. Tel.: +82 2 2123 2839; fax: +82 2 312 5375.
E-mail address: kbkim@yonsei.ac.kr (K.B. Kim).

ing polymer/CNT composite electrode is fabricated to have a three-dimensional entanglement and interconnected pores, it is expected to be an ideal electrode in terms of electronic conductivity, specific surface area, and ionic transport throughout the internal volume of the electrode via the interconnected pore structure [21–23]. Nevertheless, electrically conducting carbon additives generally have lower specific capacities than conducting polymers [24]. Therefore, it is necessary to optimize the carbon content in the composite in order to obtain high-specific capacitance and energy [25]. Recently, several methods have been reported for the preparation of CNT/PPy composite electrodes [17,26–29]. It should be noted that different values of the specific capacitance have been reported for CNT/PPy composites prepared by different methods and the measured specific capacitance has ranged from 180 to 500 F g^{-1} of the composite [13,17,26,28,29].

In this study, we report on a new and unique fabrication route to prepare CNT/PPy composite electrodes for a heavy loading of PPy of around 80 wt.% with a controlled pore size in the range of a few hundred nanometers for a pseudocapacitor application in an aqueous KCl solution. The morphological and electrochemical characterization of the CNT/PPy composites was carried out to evaluate the electrochemical utilization of the composite in pseudocapacitor applications.

2. Experimental work

2.1. Preparation of carbon nanotube/nanosize silica composite thin film substrate

Carbon nanotube (CNT) films, with a three-dimensional nanoporous network structure, were deposited on to a Pt-coated silicon wafer using an electrostatic spray deposition (ESD) technique. The process used to prepare the CNT film substrate has been described in detail elsewhere [22,23,30–32]. Multiwalled carbon nanotubes (MWNTs) were supplied from the ILJIN Nanotech Company Ltd. The nominal area of the CNT film was 1 cm × 1 cm.

In this work, we tried to control the pore size of the interconnected CNTs using nanosize silica as a sacrificial filler. First, a MWNT (effective surface area: 200 m^2 g^{-1}, ILJIN Nanotech Co. Ltd., Korea) suspension was prepared with or without nanosize silica (silicon dioxide nanopowder, 10 nm, 99.5%, Aldrich). The weight ratio of the CNTs and nanosize silica in the suspension was 1:0 (without nanosize silica), 1:10, and 1:20. The CNT suspension, with or without silica, was electrostatically sprayed downwards toward a Pt-coated silicon wafer substrate to fabricate the CNT/nanosize silica or CNT thin film. The CNT film electrode, containing silica between the entangled CNTs, was then fabricated using an electrostatic spray deposition of a mixed suspension of CNTs and nanosize silica. Later, nanosize silica was removed, leaving a three-dimensional entangled structure of a CNT film. Before removal of the silica from the CNT/silica film electrode, PPy was electrochemically deposited on to the CNTs to anchor them in their entangled structure on the removal of the silica by chemical dissolution in the HF solution. Control of the pore size of the final CNT/PPy composite film could be

achieved by changing the amount of silica in the mixed suspension of CNTs and nanosize silica. Nanosize silica successfully acted as a sacrificial filler to change the pore size of the entangled CNT film. The preparation of the CNT/nanosize silica thin film is illustrated schematically in Fig. 1.

2.2. Electropolymerization of polypyrrole on to a CNT or a CNT /nanosize silica composite thin film substrate and a Pt-coated silicon wafer

Polypyrrole was electrochemically deposited on a CNT or a CNT/silica film substrate using a potential cycling method at room temperature [25]. Although the chemical method was simple, the electrochemical method was known to be better for preparing uniform and thin films of PPy on a substrate of a complex shape with a nanoporous structure such as the CNT film substrate.
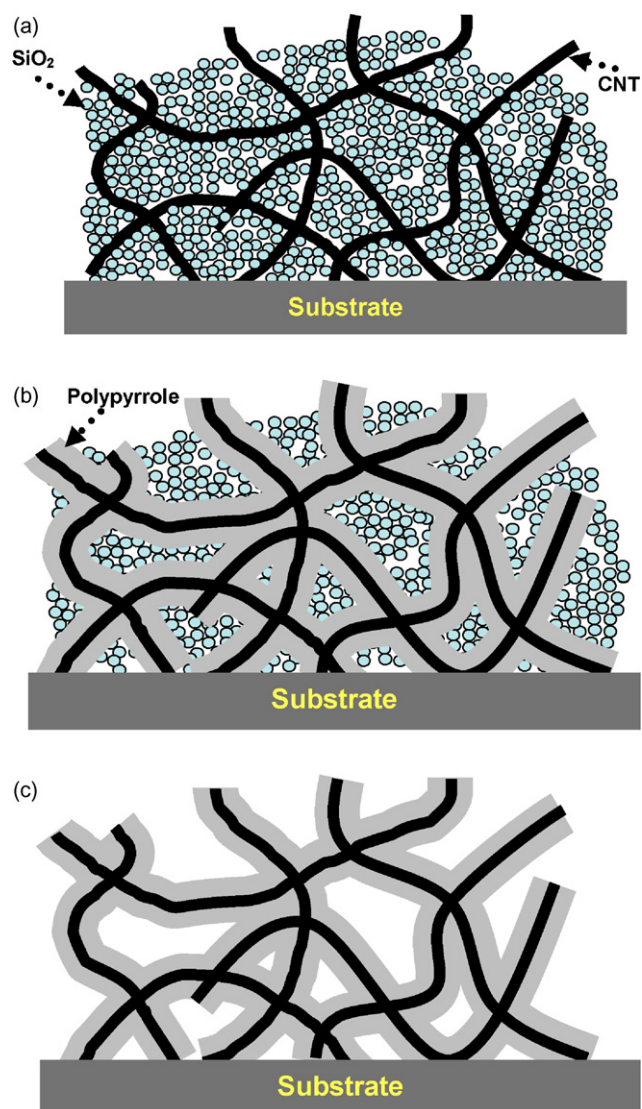

Fig. 1. Schematics of preparation of (a) as-deposited CNT/nanosized silica thin film, (b) PPy-coated CNT/nanosilica thin film, and (c) CNT/PPy thin film after removal of nanosize silica.

The aqueous polymerization electrolyte consisted of a 0.1 M pyrrole monomer (98%, Aldrich) and 0.1 M KCl. For the electropolymerization of PPy, potential cycling was carried out between 0 and 0.8 V at a potential scan rate of 50 mV s^{-1} using a potentiostat (Princeton Applied Research VMP2).

After polymerization of the PPy, the CNT/PPy or CNT/PPy/nanosize silica composite electrode was washed repeatedly with de-ionized water to remove the remaining electrolyte and monomer and dried at room temperature for 24 h. The amount of PPy was measured by weighing the difference between the bare substrate prior to PPy deposition and the PPy-deposited substrate with a microbalance (Sartorious Ultra-Microbalance, SC2). The readability and permissible tolerance of the SC2 were 0.0001 and ±0.0007 mg, respectively. Removal of the nanosize silica from the CNT/PPy/nanosize silica composite electrode was achieved by soaking the electrode in 10% HF aqueous solution for 1 h [33]. Then, the electrode was washed repeatedly with de-ionized water to remove the HF solution and dried at room temperature for 24 h.

The PPy-coated CNT film without nanosize silica is referred as CNT-NS/PPy. The PPy-coated CNT films with a weight ratio of CNT:nanosize silica of 1:10 and 1:20 are referred to as CNT-S10/PPy and CNT-S20/PPy, respectively, hereafter.

2.3. Characterization of carbon nanotube/polypyrrole composite electrodes

The morphology of the PPy-coated CNT film substrate was examined using field-emission scanning electron microscopy (FE-SEM, SIRION, FEI Company). The Raman spectra were measured using a Jobin-Yvon LabRam HR with a liquid nitrogen 2 cooled CCD multichannel detector at room temperature using conventional backscattering geometry. An argon-ion laser at a wavelength of 514.5 nm served as the laser light source.

Electrochemical measurements were made in a three-electrode electrochemical cell in which the CNT/PPy composite electrode was used as a working electrode; a platinum plate and a saturated calomel electrode (SCE) were used as the counter and reference electrodes, respectively. Cyclic voltammetry (CV) was performed using a potentiostat/galvanostat (Princeton Applied Research VMP2) in 1 M KCl aqueous solution in a potential window of −0.4 to 0.6 V. The current response in the CV curves was normalized with respect to the mass of the CNT/PPy composite.

3. Results and discussion

Fig. 2 shows scanning electron microscopic (SEM) images of the bare CNT film substrate (plane and cross-sectional views) prepared by means of ESD. It does not show any of the droplet-shape clumps often observed in binder-free CNT films prepared by other techniques [23]. This can be attributed to the formation and spraying of the tiny aerosol CNT droplets in the ESD method, as well as to the uniform dispersal of the liquid droplets on the substrate [22,23]. As shown in Fig. 2(a), the diameter of each bare CNT is approximately 15 nm with an average distance of a few tens of nanometers between the individual CNTs. Both the mass and the thickness of the CNT film increase lin-
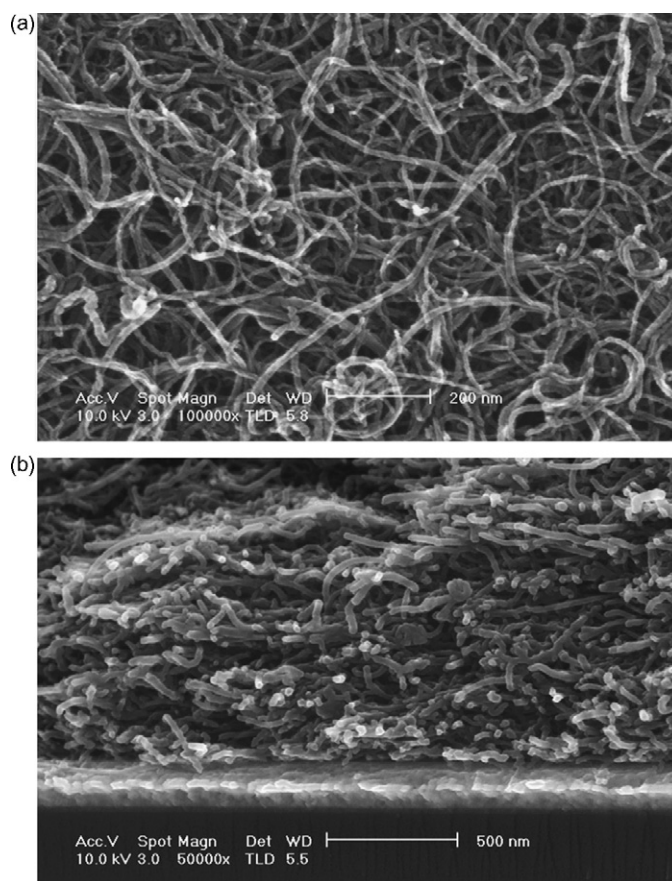

Fig. 2. SEM images of bare CNT film substrate: (a) plane and (b) cross-sectional views.

early with increase in the amount of spray solution. The CNTs, in the CNT film substrate, are entangled and interconnected to form a uniform film with a three-dimensional porous structure at the nanometer scale. This meets the requirements of an ideal substrate for pseudocapacitor applications in terms of electronic conductivity, specific surface area, and an interconnected pore structure.

Fig. 3 shows SEM images of the PPy coated on the three different CNT film substrates after removal of the silica from the films (insets of Fig. 3a, c, and e have magnification of 50 000×); with a PPy loading of 77.2 wt.% for CNT-NS/PPy in Fig. 3a and b, a PPy loading of 82.2 wt.% for CNT-S10/PPy in Fig. 3c and d, and a PPy loading of 83.4 wt.% for CNT-S20/PPy in Fig. 3e and 3f. The amount of CNTs was about 0.07 mg for each of the electrodes. A HRTEM image shows that the PPy is coated heterogeneously and uniformly on the substrate of the CNTs film by electrochemical deposition (data not shown). The average diameter of the nanotubes after electrodeposition of the PPy is 50 nm. It is clear from the cross-sectional views of the CNT/PPy composites that the three-dimensional nanoporous CNT substrates are coated entirely with PPy throughout their entire thickness. Fig. 3a and b presents plane and cross-sectional views of the CNT-NS/PPy composite electrode without nanosize silica, respectively. The PPy is deposited over the entire CNT film substrate with nearly all the pores filled with PPy. This produces a film of PPy having CNTs embedded inside that
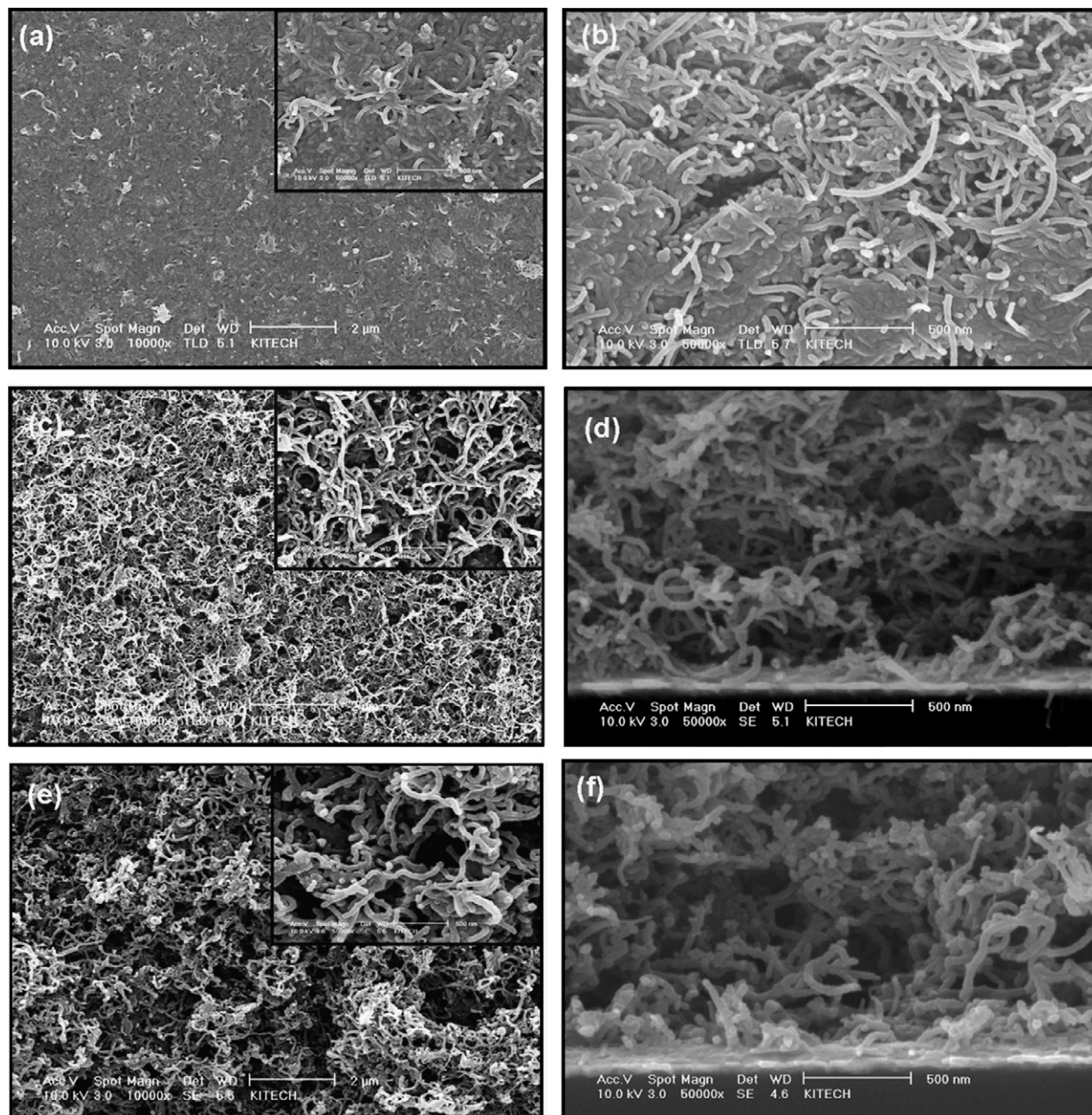
Fig. 3. Plane and cross-sectional SEM images: (a) and (b) for 77.2 wt.% PPy coated on CNT film prepared without nanosize silica (CNT-NS/PPy); (c) and (d) for 82.2 wt.% PPy coated on CNT film prepared with nanosize silica (CNT-S10/PPy; CNT:silica = 1:10); (e) and (f) for 83.4 wt.% PPy coated on CNT film prepared with nanosize silica (CNT-S20/PPy; CNT:silica1 = 1:20).

thereby loses the nanoporous nature of the CNT film substrate. The thickness and density of the CNT film in the CNT-NS/PPy composite are about 1.89 μm and 0.353 g cm^{-3}, respectively.

Fig. 3c and d gives plane and cross-sectional views of the CNT-S10/PPy composite electrode (weight ratio of CNT to nanosize silica, 1:10), respectively, with an average distance of 100–200 nm between the individual CNTs. As shown in Fig. 3c and d, the pores in the CNT/PPy film substrate are not blocked by any polypyrrole deposit, even for a heavy loading of 82.2 wt.% PPy on the CNTs. We clearly demonstrate that nanosize silica successfully acts as a sacrificial filler in the CNT/nanosize silica thin film and contributes effectively to the enlargement of the pore size of the entangled CNTs in the film. As a result, the

nanoporous structure of the CNT-S10/PPy composite electrode is still well maintained. The thickness and the density of the CNT film of the CNT-NS/PPy composite are 8 μm and 0.082 g cm^{-3}, respectively.

Fig. 3e and f shows the plane and cross-sectional views of the CNT-S20/PPy composite electrode (weight ratio of CNT to nanosize silica, 1:20), respectively, with an average distance of 400 nm between the individual CNTs. As shown in Fig. 3e and f, the pores in the CNT/PPy film substrate are clearly visible without any pore filling with a polypyrrole deposit even for a high loading of 83.4 wt.% PPy coating on the CNTs. The thickness and the density of the CNT film in the CNT-S20/PPy composite are 15 μm and 0.040 g cm^{-3}, respectively.

Table 1
Thickness and density of CNT film in CNT/PPy composites for various ratios of CNT and nanosized silica

	Ratio of CNT to nanosize silica	Thickness of CNT film in CNT/PPy film (μm)	Density of CNT film in CNT/PPy film (g cm^{-3})
CNT-NS	1:0 (without silica)	1.89	0.353
CNT-S10	1:10	8.0	0.082
CNT-S20	1:20	15.0	0.040

These results demonstrate that the nanoporous structure of the CNT film substrate can be well maintained in the CNT/PPy composite electrode with a heavy loading of PPy approaching 80 wt.% only through enlargement of the average distance between the individual CNTs. Table 1 lists the thickness and density of the three different CNT films prepared at different ratios of CNT and nanosize silica. The thickness of the CNT films increases in proportion to the amount of nanosize silica in the suspension of CNT and silica. Accordingly, the density of the CNT films decreases with increase in nanosize silica in the suspension.

Fig. 4 presents the Raman spectra of the pure PPy, bare CNT and the CNT/PPy composite after silica removal in the HF solution. The typical peak of pure CNT at 1591 cm^{-1} can be attributed to the graphite wall [34]. The band at 1334 cm^{-1} is assigned to slightly disordered graphite [35]. For pure PPy, the strong peak at 1589 cm^{-1} represents the backbone stretching mode of the C=C bonds. The band located at approximately 1417 cm^{-1} is assigned to the C–N stretching mode [36]. The peak at approximately 1048 cm^{-1} is assigned to the C–H in plane deformation and the peak at approximately 1330 cm^{-1} to the ring-stretching mode of PPy [37,38]. The bands at approximately 930 and 987 cm^{-1} are assigned to the ring deformation associated with the di-cation (di-polaron) and radical cation (polaron), respectively [39–41]. For the CNT/PPy composite, however, no extra peaks are observed in the Raman spectra except for the characteristic peaks of CNT and PPy. This suggests that no new chemical bonds are formed between the CNTs and PPy in the CNT/PPy composite and no chemical changes in PPy in the composite after removal of silica with HF.
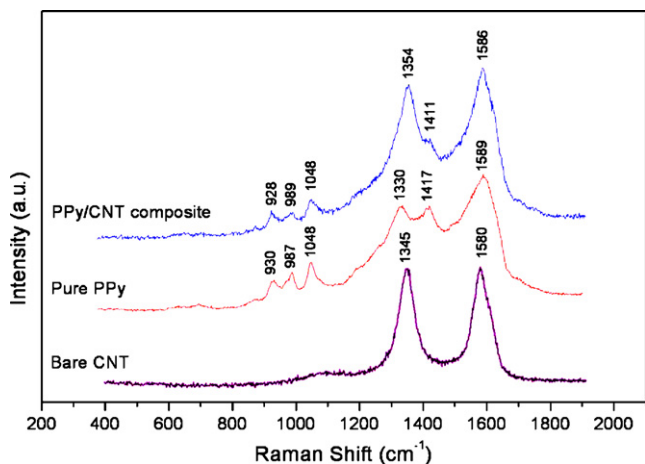

Fig. 4. Raman spectra of bare CNT, pure PPy, and CNT/PPy composite electrodes after silica removal.

Fig. 5a–c gives the cyclic voltammograms (CVs) of the three different CNT/PPy composite films prepared at different ratios of CNT and nanosize silica measured as a function of the potential scan rate in a 1 M KCl solution. The scan rate was varied from 10 to 500 mV s^{-1} in order to evaluate the high-rate capability of the electrodes in a potential window of −0.4 to 0.6 V. In this study, the current value in the CV curves is normalized with respect to the mass of the CNT/PPy composite.

The CNT-NS/PPy composite electrode yields rectangular-shaped CVs only at slow scan rates, as shown in Fig. 5a. The CVs of the CNT-NS/PPy composite electrode become extremely distorted in shape as the potential scan rate is increased up to 500 mV s^{-1}, which implies a poor high-rate capability of the electrode. This behaviour is closely related to the microstructure of the CNT-NS/PPy electrode with its pores filled with PPy losing the nanoporous nature of the CNT film substrate in Fig. 3a and b.

In Fig. 5b and c, the CNT-S10/PPy and CNT-S20/PPy composite electrodes are seen to have featureless, rectangular-shaped CVs at all potential scan rates with a steep change in the current flow direction at each potential limit. This suggests that the typical pseudocapacitive behaviour of the CNT-S10/PPy and CNT-S20/PPy composites is maintained, even at a high potential scan rate of 500 mV s^{-1}. This indicates that the pseudocapacitive reactions of PPy in the CNT-S10/PPy and CNT-S20/PPy composite electrodes are highly reversible. The microstructures of the CNT-S10/PPy and CNT-S20/PPy composites with the nanoporous nature of the CNT film substrate in Fig. 3c, d and Fig. 3e, f can explain the improved high-rate capability observed in Fig. 5b, c.

Fig. 6a and b shows the scan-rate dependence of the specific and normalized capacitance of the three CNT/PPy composite electrodes. The specific capacitance is determined from the voltammetric charge using the following equation:

$$C_p = \frac{q_a + |q_c|}{2m\Delta V} \qquad (1)$$

where C_p, q_a, q_c, m, and ΔV are the specific capacitance, the anodic and cathodic charges on the anodic and cathodic scans, the mass of the total electrode, and the potential range of the CV, respectively [4,5]. The specific capacitances of the CNT-NS/PPy, CNT-S10/PPy, and CNT-S20/PPy composite electrode are 176, 240 and 250 F g^{-1} at 10 mV s^{-1}, respectively. The specific capacitances of the CNT-S10/PPy and CNT-S20/PPy electrodes are expected to be similar because of their typical microstructure characterized by their nanoporous nature. The relatively low specific capacitance of the CNT-NS/PPy composite electrode can be attributed to the lower electrochemical utilization of PPy in the CNT-NS/PPy due to the lack of specific
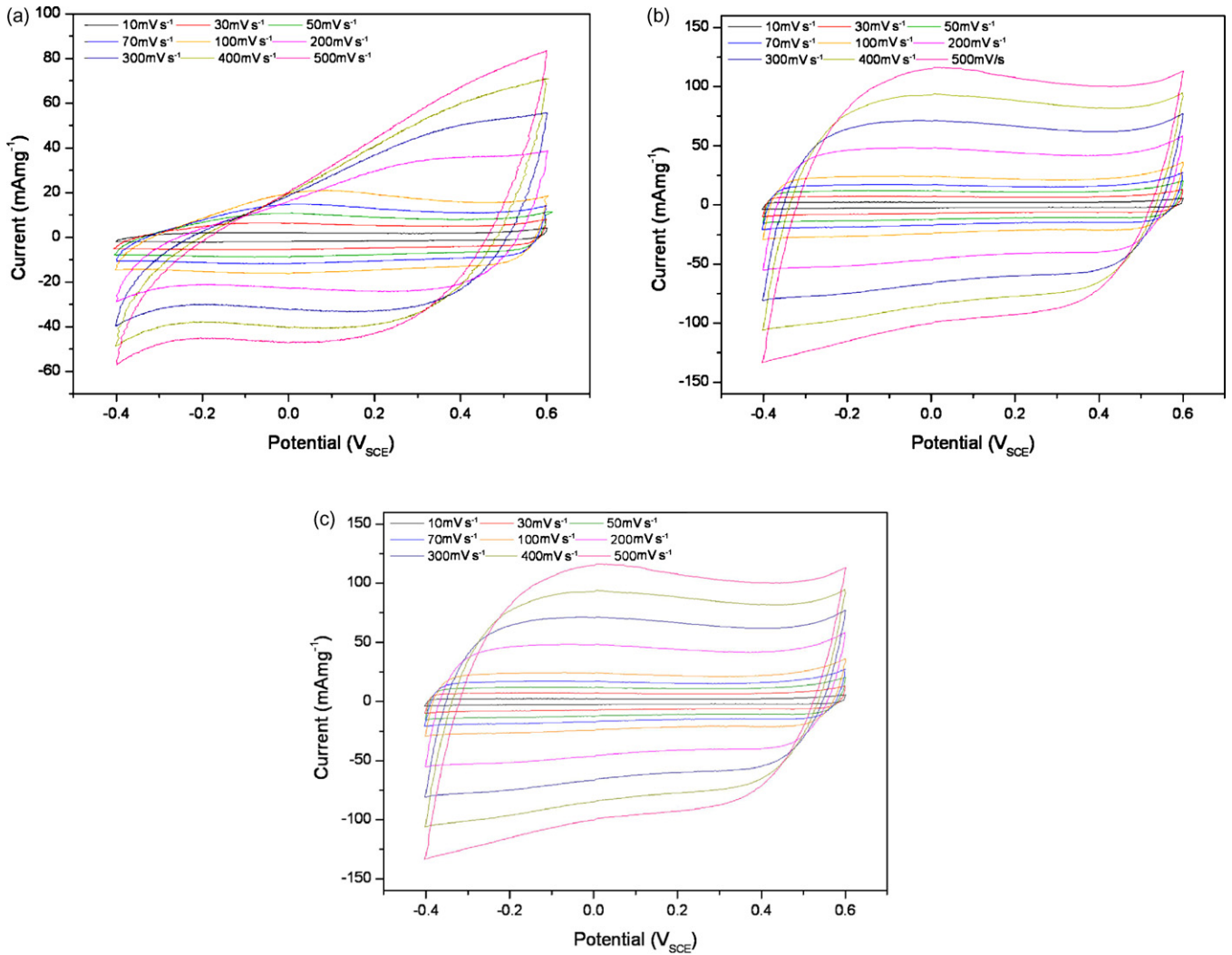
Fig. 5. Cyclic voltammograms for (a) CNT-NS/PPy, (b) CNT-S10/PPy, and (c) CNT-S20/PPy composite electrodes, respectively.
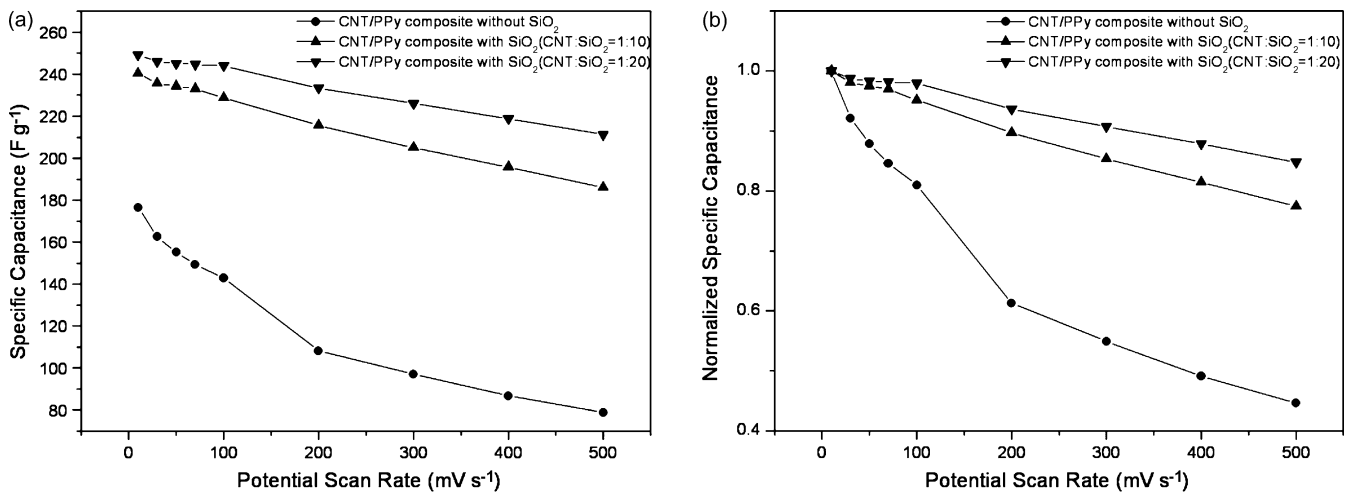

Fig. 6. (a) Specific and (b) normalized capacitance of CNT-NS/PPy (●), CNT-S10/PPy (▲), and CNT-S20/PPy (▼) composite electrodes at various potential scan rates (per composite mass).

surface area and interconnected pore structure in the electrode. The specific capacitance decreases with increasing scan rate from 10 to 500 mV s^{-1} for each of the electrodes.

Fig. 6b shows the normalized capacitance of the three CNT/PPy composite films prepared at different ratios of CNT and nanosize silica as a function of the potential scan rate. The normalized capacitance is obtained by dividing the specific capacitance at each potential scan rate by that measured at 10 mV s^{-1}. The normalized specific capacitances of the CNT-S10/PPy and CNT-S20/PPy composite decrease by 20% and 15% at a potential scan rate of 500 mV s^{-1}, respectively. By contrast, it decreases by 55% for the CNT-NS/PPy composite at a potential scan rate of 500 mV s^{-1}. The CNT-S10/PPy and CNT-S20/PPy composite electrodes exhibit better high-rate capability than the CNT-NS/PPy composite electrode. The change in the specific capacitance and high-rate capability can be attributed to a change in the morphology of the CNT/PPy composite.

In summary, high-specific capacitance and good high-rate capability of CNT/PPy composite electrodes can be achieved only when the electrode is fabricated to have a large specific surface area, high-electronic conductivity, and facile ionic transport throughout the internal volume of the electrode via an interconnected pore structure on the nanometer scale.

4. Conclusions

A new and unique fabrication route, which uses electrostatic spray deposition of a mixed suspension of CNTs and nanosize silica is developed to fabricate CNT/PPy composite electrodes with a heavy loading of PPy of around 80 wt.% for a pseudocapacitor application. The pore size is controlled in the range of a few ten to a few hundred nanometers. The nanosize silica successfully acts as sacrificial filler. The pore size in the CNT/PPy composite can be controlled by changing the relative amount of the nanosize silica in the suspension. The specific capacitance of a CNT/PPy composite with 83.4 wt.% polypyrrole is 250 F g^{-1} at a potential scan rate 10 mV s^{-1} in 1 M KCl and it decreases by 15% to 211 F g^{-1} at 500 mV s^{-1}. A high-specific capacitance and good high-rate capability of the CNT/PPy electrode can be achieved through fabrication of the composite electrode with the characteristics of large specific surface area, high-electronic conductivity, and facile ionic transport throughout the internal volume of the electrode via an interconnected pore structure on the nanometer scale.

Acknowledgements

References

[1] K.S. Ryu, K.M. Kim, N.G. Park, Y.J. Park, S.H. Chang, J. Power Sources 103 (2002) 305.
[2] A.M. White, R.C.T. Slade, Synth. Met. 139 (2003) 123.
[3] V. Srinivasan, J.W. Weidner, J. Electrochem. Soc. 144 (1997) L210.
[4] K.W. Nam, K.B. Kim, Electrochemistry 69 (2001) 467.
[5] K.W. Nam, K.B. Kim, J. Elelctrochem. Soc. 149 (2002) A346.
[6] C.C. Hu, T.W. Tsou, Electrochem. Commun. 4 (2002) 105.
[7] J.P. Zheng, P.J. Cygan, T.R. Jow, J. Electrochem. Soc. 142 (1995) 2699.
[8] I.H. Kim, K.B. Kim, J. Electrochem. Soc. 151 (2004) E7.
[9] C.C. Hu, X.X. Lin, J. Electrochem. Soc. 149 (2002) A1049.
[10] C.C. Hu, J.Y. Lin, Electrochim. Acta 47 (2002) 4055.
[11] M. Mastragostino, C. Arbizzani, F. Soavi, Solid State Ionics 148 (2002) 493.
[12] F. Fusalba, P. Gouerec, D. Villers, D. Belanger, J. Electrochem. Soc. 148 (2001) A1.
[13] K. Jurewicz, S. Delpeux, V. Bertagna, F. Beguin, E. Frackowiak, Chem. Phys. Lett. 347 (2001) 36.
[14] S. Sadki, P. Schottland, N. Brodie, G. Sabouraud, Chem. Soc. Rev. 29 (2000) 283.
[15] L. Jiang, J. Liu, D. Wu, H. Li, R. Jin, Thin Solid Films 503 (2006) 241.
[16] R. Kotz, M. Carlen, Electrochim. Acta 45 (2000) 2483.
[17] V. Khomenko, E. Frackowiak, F. Beguin, Electrochim. Acta 50 (2005) 2499.
[18] E. Frackowiak, Phys. Chem. Chem. Phys. 9 (2007) 1774.
[19] V. Mottaghitalab, B. Xi, G.M. Spinks, G.G. Wallace, Synth. Met. 156 (2006) 796.
[20] T. Wu, S. Lin, J. Poly. Sci. B: Poly. Phys. 44 (2006) 1413.
[21] J.H. Park, J.M. Ko, O.O. Park, J. Electrochem. Soc. 150 (2003) A864.
[22] J.H. Kim, K.W. Nam, K.B. Kim, Korean Patent 2004/10-2004-0099039 (2004).
[23] J.H. Kim, K.B. Kim, Carbon 44 (2006) 1963.
[24] E. Frackowiak, V. Khomenko, K. Jurewicz, K. Lota, F. Begun, J. Power Sources 153 (2006) 413.
[25] I.H. Kim, J.H. Kim, Y.H. Lee, K.B. Kim, J. Electrochem. Soc. 152 (2005) A2170.
[26] M. Hughes, G.Z. Chen, M.S.P. Shaffer, D.J. Fray, A.H. Windle, Compos. Sci. Technol. 64 (2004) 2325.
[27] J.H. Chen, Z.P. Huang, D.Z. Wang, S.X. Yang, W.Z. Li, J.G. Wen, Z.F. Ren, Synth. Met. 125 (2002) 289.
[28] K.H. An, K.K. Jeon, J.K. Heo, S.C. Lim, D.J. Bae, Y.H. Lee, J. Electrochem. Soc. 149 (2002) A1058.
[29] M. Hughes, M.S.P. Shaffer, A.C. Renouf, C. Singh, G.Z. Chen, D.J. Fray, A.H. Windle, Adv. Mater. 14 (2002) 382.
[30] K.W. Nam, E.S. Lee, J.H. Kim, Y.H. Lee, K.B. Kim, J. Electrochem. Soc. 152 (2005) A2123.
[31] I.H. Kim, J.H. Kim, B.W. Cho, K.B. Kim, J. Electrochem. Soc. 153 (2006) A989.
[32] I.H. Kim, J.H. Kim, B.W. Cho, K.B. Kim, J. Electrochem. Soc. 153 (2006) A1451.
[33] R. Guo, G. Li, W. Zhang, G. Shen, D. Shen, Chem. Phys. Chem. 6 (2005) 2025.
[34] H. Hlura, T.W. Ebbesen, T. Tanigaki, H. Takahashi, Chem. Phys. Lett. 202 (1993) 509.
[35] X.Y. Tao, X.B. Zhang, L. Zhang, J.P. Cheng, F. Liu, J.H. Luo, J.Q. Luo, H.J. Geise, Carbon 44 (2006) 1425.
[36] M. Bazzaoui, L. Martins, E. Bazzaoui, J. Martins, J. Electroanal. Chem. 537 (2002) 47.
[37] Y.C. Liu, B.J. Hwang, Synth. Met. 113 (2000) 203.
[38] Y.C. Liu, B.J. Hwang, W.J. Jian, R. Santhanam, Thin Solid Films 374 (2000) 85.
[39] Y. Furukawa, S. Tazawa, Y. Fujii, I. Harada, Synth. Met. 24 (1988) 329.
[40] J. Duchet, R. Legras, S. Demoustier-Champagne, Synth. Met. 98 (1998) 113.
[41] A.B. Goncalves, A.S. Mangrich, A.J.G. Zarbin, Synth. Met 114 (2000) 119.